PAPER • OPEN ACCESS

Numerical investigation of a Pelton turbine at several operating conditions

View the article online for updates and enhancements.

Numerical investigation of a Pelton turbine at several operating conditions

Saroj Gautam[1, *], Sailesh Chitrakar[1], Hari Prasad Neopane[1], Bjørn W Solemslie[2] and Ole Gunnar Dahlhaug[2]

[1]*Turbine Testing Lab, Kathmandu University, Dhulikhel, Kavre*
[2]*Department of Energy and Process Engineering, NTNU, Norway*
* Corresponding author: saroj.gautam2019@hotmail.com

Abstract. The use of Computational Fluid Dynamics (CFD) for predicting the flow behaviour in Pelton turbines is limited by the complex nature of the flow, interaction between the jets and interference of the water after the impact on the buckets. Besides, validation of the numerical results in such turbines is usually challenging due to the unsteadiness of the flow properties. Hence, time-dependent analysis with multi-phase models is required for obtaining such solutions. This paper conducts a CFD analysis on a Pelton turbine using RANS based Eulerian scheme. The fluid domain consists of three successive buckets placed in their corresponding circumferential locations, along with a spear valve, which is adjusted for various operating conditions. Such a domain assumes that the interaction of the jet on the buckets takes place for a maximum of three buckets at any particular time. The results of the CFD analysis are compared with the experimental results for all the studied opening conditions. The objective of this work is to build a suitable numerical model that can be applied to any Pelton turbines, such that a complete performance curve of the turbine can be generated. The flow pattern between entry and exit of the bucket obtained from CFD is compared with images taken from a high speed camera in rotating frame of reference. The results of the numerical analysis are found to be in a good agreement with the experimental data.

Keywords: Computation Fluid Dynamics, Pelton Turbine, Numerical Analysis, Experimental Data

1. Introduction

Within the last few decades, the use of computational techniques has grown widely in the field of hydraulic turbines, due to its possibility of predicting the flow field more conveniently than the experimental methods. However, in terms of the types of turbines, the use of CFD for reaction turbines is found to be more popular due to the complexities in the numerical model made for the impulse turbines. These complexities are caused by the unsteady multiphase flow field, interaction of the jet and the buckets and free surface flows which makes the flow highly unpredictable. However, with the advancement in the computational capacity, the numerical studies in Pelton turbines have flourished in the past few years. Today, there is a possibility to choose a 3D simulation in the complete turbine, including runner, nozzle and manifolds [1], or use a simplified technique considering the rotational and translational periodicity options of the turbine [2]. Some CFD codes can also incorporate Lagrangian approach, which can be more relevant for studying the free surface flows of the Pelton turbines [3,4]. For Eulerian schemes, the reduced computational domain, i.e. half bucket and rotational periodicity approaches are found to be used more predominantly, in order to reduce the number of the mesh and conduct an in-depth analysis over a chosen volume [5-8].

The validation of the numerical results in the case of Pelton turbines is one of the major issues that needs to be addressed. Because of the complicated bucket shapes, the flexibility of using the high quality structured grids in the fluid domain is restricted. In such cases, the experimental validation of the numerical results on the basis of the performance of the turbines, i.e. torque, mechanical power and efficiency of the turbine can be one of the methods to increase the reliability of CFD. In this study, a laboratory scale of a Pelton turbine is chosen for the CFD study, such that a proper validation of the numerical result can be carried out by comparing it with the experimental result.

2. Numerical model

The numerical model chosen for this study consists of two domains, stationary and rotating. The stationary domain consists of the spear valve, which produces a jet that is carried into the runner. The stationary domain also consists of an extended region, whose circumferential length matches with that of the rotating domain. In this study, three full buckets were taken inside the rotating domain, out of the 23 buckets present in the actual runner. The three buckets were chosen based on an assumption that the interaction of the jet and the buckets take place for maximum three buckets at a time. For example, if there are four buckets namely B1, B2, B3 and B4 placed successively, the jet starts to interact with B1 at first. Later, when the jet interacts with B2, some portion of the jet also interacts with B1 and B3. As the jet stops to interact with B1, some portion of the jet starts interacting with B4. The net torque produced on the runner can also be measured based on this combined interaction between the jet and the buckets. Hence, the net power output from the runner is a result of the jet interacting with 3 buckets at any instant of time. In the rotating domain, the circumferential length is extended on both sides of the bucket so that a well-developed flow is formed before the first bucket comes in contact with the jet.

This study uses RANS based Eulerian scheme with a time dependent analysis. The analysis consists of two sets of the transient solutions. The first transient solution is to ensure that the flow has entered the runner with a well-developed jet. The time step for the first solution was chosen to be 1 revolution per step with 20 revolutions, since the velocity of the flow at the inlet was low due to large diameter of the pipe. The total time step in general can be selected on the basis of the following equation:

$$T_1 = \frac{60}{N} \times n = \Delta t_1 \times n$$

Where N = revolution per minute of the runner and n = number of revolutions
T_1 = total time of simulation and Δt_1 = time step for the first simulation

Whereas the first transient solution was initialized by considering the fluid at rest, the second transient simulation takes the final parameters of the first solution as the initial values. In this case, an offset in the interface between the rotating and the stationary domain was maintained to be 60º, such that the jets would hit the buckets gradually as the simulation progresses. The total time of simulation in this case was chosen as the time needed for the runner to complete 60º rotation and the time step of 1º, i.e.,

$$T_2 = \frac{60}{N} \times \frac{60}{360}$$
$$\Delta t_2 = \frac{60}{N} \times \frac{60}{360} \times \frac{1}{60}$$

A multiphase flow with air-water mixture was incorporated in the model. The initial values of the volume fractions of air and water for the first transient simulation was chosen to be 1 and 0 respectively. This was to ensure that there is no water in the domain during the start-up.

The stationary domain consists of an inlet, where the mass flow rate of the flow corresponding to the spear valve opening was defined. This mass flow rate was obtained from the experiment, corresponding to a particular spear valve opening. This study compares the results of 7 conditions from 6 mm to 18 mm spear valve opening compared to the closed condition. The spear valve and the pipe surrounding the flow passage in the stationary domain were defined as no-slip walls. A transient rotor-stator interface was defined on the surface connecting the two domains. The pitch ratio in this case was 1, because the two surfaces were coinciding. In this study, the rotational speed of the runner was chosen to be 628 rpm for all the openings and the corresponding experimental results for the same speed was compared.

The rotating domain consists of the interface towards its inlet. It also consists of the buckets, which were defined as no-slip walls. The side surfaces of this domain were defined as opening, with atmospheric pressure and the volume fractions of air and water as 1 and 0 respectively. The total boundary conditions used for the CFD analysis is shown in Figure 1. The rotation of the runner in the figure is in a clockwise direction.

All simulations were performed using SST turbulence model. The domains were discretized using hybrid mesh, with hexahedral inflation layers near the wall boundaries. The commercial CFD solver ANSYS-CFX-18.1 was used for numerical simulations. The simulations used high-resolution discretization in advection scheme and first order upwind scheme in turbulence equations.
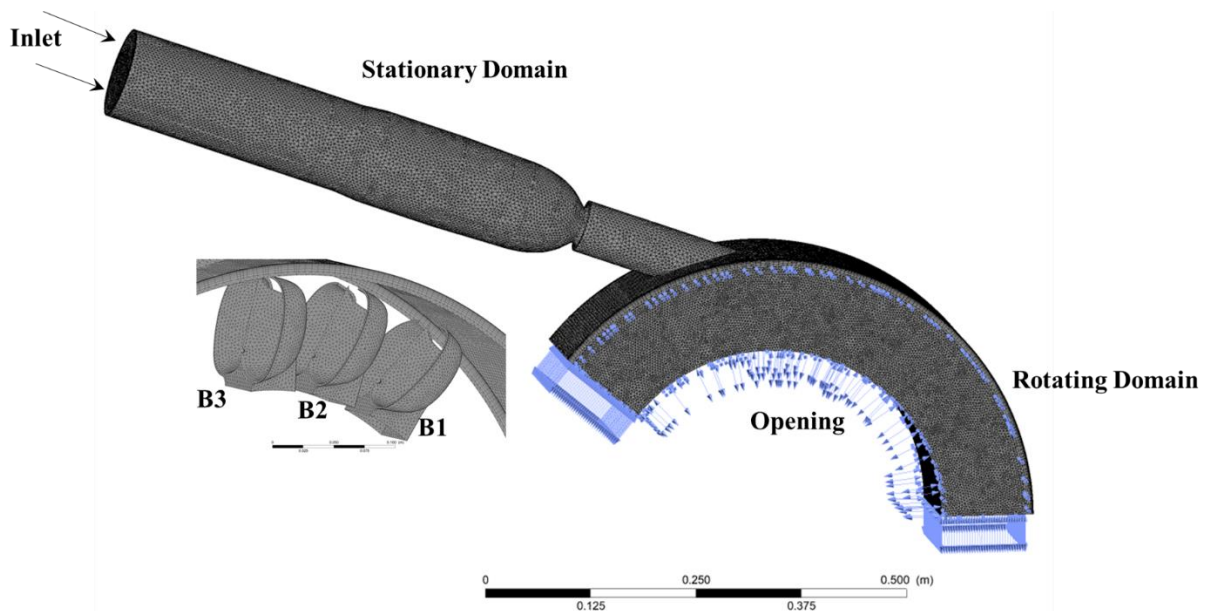

Figure 1. Domain, mesh and boundary conditions used for CFD

3. Results and discussion

The torque on each bucket along the axis of its rotation was monitored during the simulation. As the jet interacted with the bucket B1, the force applied on the bucket due to the jet induces a torque, which grows as more water strikes on the bucket surface. When the torque on the first bucket B1 reaches the maximum value, some part of the jet also interacts with the second bucket B2, which produces torque on this bucket. When the jet is about to leave B1, some part of the jet also start to strike the third bucket B3. At this instant, the torque produced on the runner is the sum of the torque produced on all three buckets. The net torque from the runner remains steady as the jet interacts with the consecutive buckets during its rotation. However, since this study consists of only three buckets, the torque gradually decreases as the jet begin to stop interacting with any of the buckets.

The resulting rotation vs the torque produced on the buckets can be seen in Figure 2. The values correspond to 12 mm spear valve opening. The graphs could be on the positive or negative side of y-axis depending upon the direction of the rotation. The total torque produced on the runner stays around 225 Nm, which can be considered as the average torque from the turbine. A small counter torque can be noticed at the start of the torque produced on each bucket. This is due to the jet hitting the back side of the bucket as the first interaction zone.

The net torque, as shown in Figure 2 can be obtained for all the opening conditions. These values are the average of the total torque after a steady solution is achieved. In Figure 3, the comparison of the torque obtained from CFD and the experiment is shown. The experimental results are obtained from the experimental rig of Waterpower Lab at Norwegian University of Science and Technology. The coarse mesh contained a total of around 2.3 million elements in the complete domain, whereas the fine mesh contained around 5 million elements. It can be seen that the predicted torque depends on the size of the mesh. For coarse mesh, the value of the torque is under-predicted as compared to the experimental results. However, for the fine mesh, estimated torque from CFD is higher than that of the experiment for all the conditions. This difference might be due to the losses in experiments which were not incorporated in CFD.
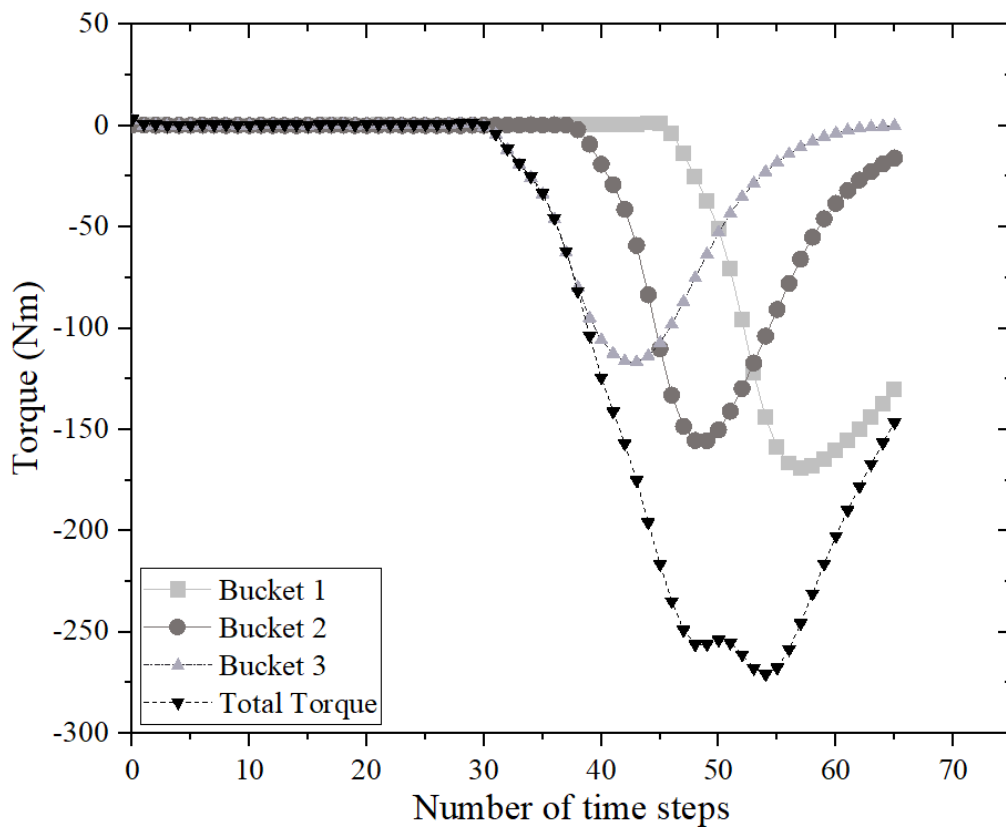
Figure 2. Torque produced on the buckets along the rotation of the runner
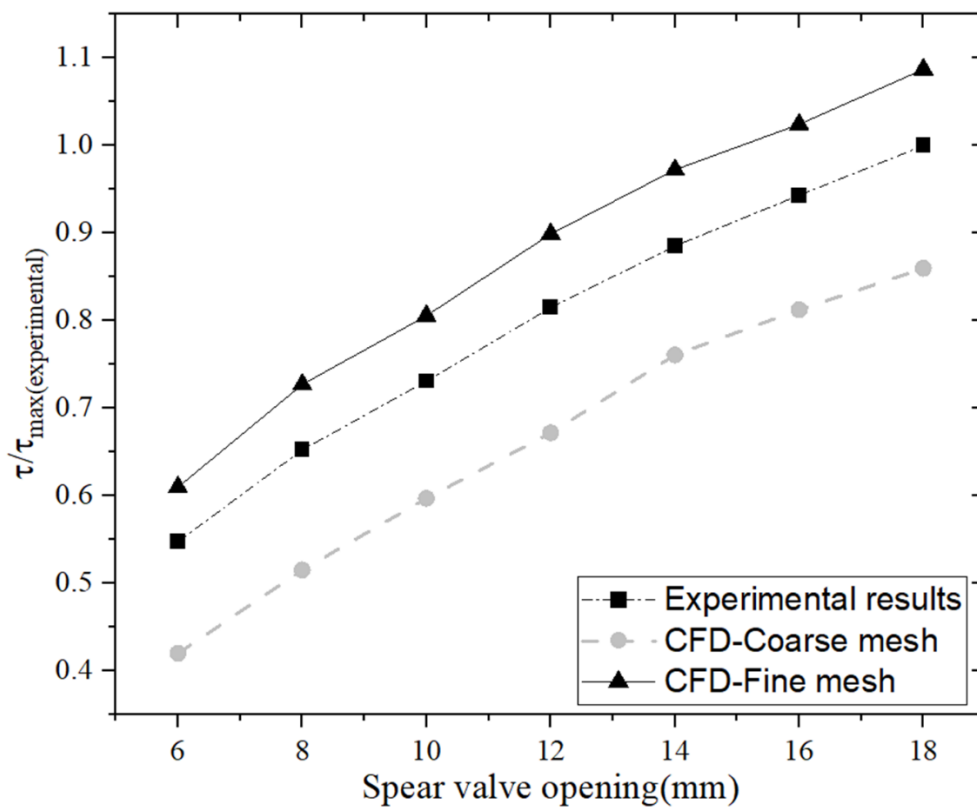

Figure 3. Net torque at different spear valve opening conditions

It was found that the deviation in the estimation of the torque depends significantly on the quality of the jet formed downstream of the spear valve. Figure 4 shows the water volume fraction downstream of the spear valve at three planes, which are 4 cm apart from each other. At coarse mesh, the jet is not properly resolved, which results in increase in the jet diameter. However, in this figure, it can be seen that the jet is properly resolved before entering the runner.
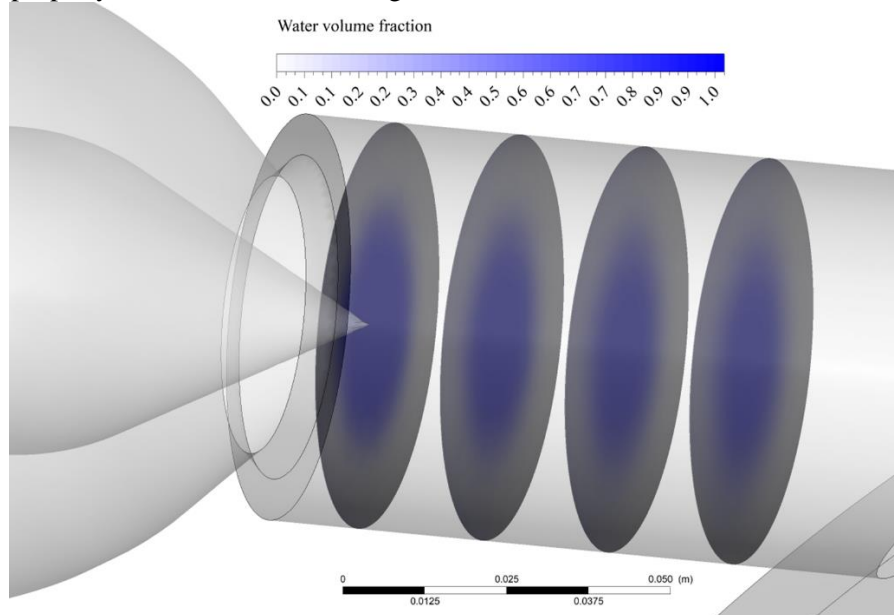

Figure 4. Path of the jet downstream of the spear valve

The flow visualization through CFD in Pelton turbines can be done in several ways. One of the common techniques is the use of iso-surfaces or volumes, so that the flow deviating away from the splitters can be observed conveniently. Figure 5 shows the iso-surface of the water volume fraction at 0.3 with the water velocity in that surface. At this instant, the maximum torque is achieved for B2. It can be seen from this figure that at this instant, the water jet interacts with all three buckets and hence, the net torque is achieved from all three interactions.
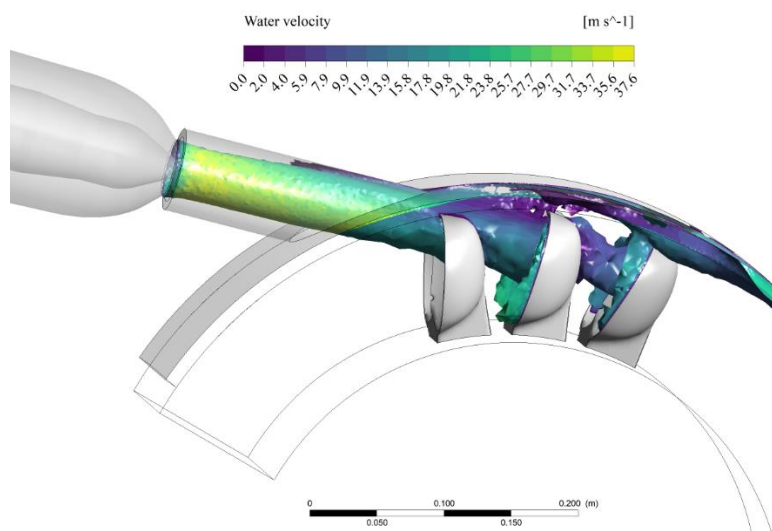

Figure 5. Iso-surface of the water volume fraction at the value 0.3 with water velocity

A closer view of the iso-surface is shown in Figure 6. At this instant, the result of the CFD is compared with that from the experiment. The experimental results in this case are in the form of pictures obtained from a high speed camera during the turbine's operation. The distribution of the flow

around the buckets obtained from the two methods is found to be comparable. At this instant, the water has started to hit the front bucket, whereas it has started to leave the rear one. During this time, the water splash is more predominant at the rear side, whereas more streamlined towards the front side. The division of the water towards the two sides of the splitter can also be observed from the two pictures. The splash seen in the experiment, which is outside the bucket is not seen in this figure from CFD because the volume fraction of water at those regions is much less than 0.3.
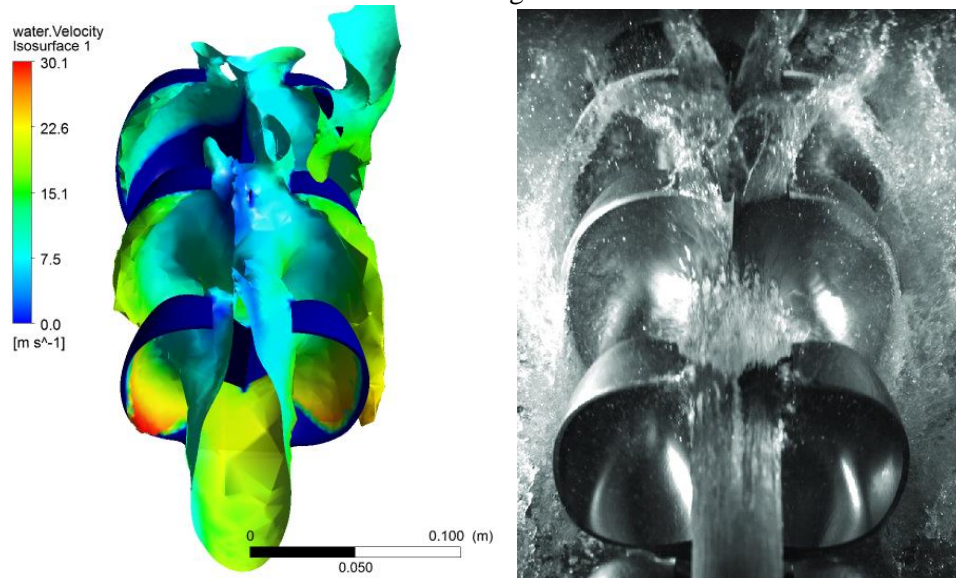

Figure 6. Iso-surface of the water volume fraction compared with the experiment [9]

4. Conclusion
A numerical investigation of a laboratory scale Pelton turbine is carried out in this study. The results of the CFD are compared with the experiment. The fluid domain for CFD contained a stationary domain with the spear valve and a rotating domain with three buckets. The simulations contained 7 opening conditions of the spear valve with their corresponding flow rates at a constant rotational speed. The results of the numerical analysis were found to be dependent on the size of the mesh, especially at the regions downstream of the valve. The trend of the torque versus the opening conditions was found to be comparable between the experiment and CFD for both coarse and fine mesh. However, values of the torque in the runner predicted by the fine mesh were found to have a closer match compared to the experiment. Also, the flow distribution around the buckets was found to have close agreement with the picture taken during the experiment.

5.Acknowledgement

6. References
[1] Zeng C J, Xiao Y X, Luo Y Y, Zhang J, Wang Z W, Fan H G and Ahn S H 2018, Hydraulic Performance Prediction of a Prototype Four-Nozzle Pelton turbine by Entire Flow Path Simulation, Renewable Energy, doi: 10.1016/j.renene.2018.02.075

[2] Nigussie T, Engeda A and Dribssa E 2017, Design, Modeling and CFD Analysis of a Micro Hydro Pelton Turbine Runner: For the Case of Selected Site in Ethiopia, International Journal of Rotating Machinery, Vol. 2017, 3030217

[3] Leguizamon S, Jahanbakhsh E, Alimirzazadeh S, Maertens A and Avellan F 2019, Multiscale Simulation of the Hydroabrasive Erosion of a Pelton Bucket: Bridging Scales to Improve the Accuracy, International Journal of Turbomachinery Propulsion and Power, Vol. 4(9)

[4] Leguizamon S, Jahanbakhsh E, Maertens A, Alimirzazadeh S and Avellan F 2019, Simulation of the hydroabrasive erosion of a bucket: A multiscale model with projective integration to circumvent the spatiotemporal scale separation, IOP Conference Series: Earth and Environmental Science, Vol. 240, 072014

[5] Batbeleg T and Lee Y H 2018, Numerical prediction of the performance of a micro class Pelton turbine, IOP Conference Series: Earth and Environmental Science 163, 012058

[6] Kumashiro T, Fukuhara H and Tani K 2016, Unsteady CFD simulation for bucket design optimization of Pelton turbine runner, IOP Conference Series: Earth and Environmental Science 49, 022003

[7] Santolin A, Cavazzini G, Ardizzon G and Pavesi G 2009, Numerical investigation of the interaction between jet and bucket in a Pelton turbine, Proceedings of the Institution of Mechanical Engineers, Part A: Journal of Power and Energy, Vol. 223, 721

[8] Chitrakar S, Solemslie B W, Neopane H P and Dahlhaug O G 2020, Review on numerical techniques applied in impulse hydro turbines, Renewable Energy 159, 843-859

[9] Solemslie B W 2016, Experimental methods and design of a Pelton bucket, PhD Thesis